

This is an Open Access document downloaded from ORCA, Cardiff University's institutional repository:<https://orca.cardiff.ac.uk/id/eprint/116058/>

This is the author's version of a work that was submitted to / accepted for publication.

Citation for final published version:

Perkins, Russell J., Shoemaker, Richard K., Carpenter, Barry K. and Vaida, Veronica 2016. Chemical equilibria and kinetics in aqueous solutions of zymonic acid. *Journal of Physical Chemistry A* 120 (51) , pp. 10096-10107. 10.1021/acs.jpca.6b10526

Publishers page: <http://dx.doi.org/10.1021/acs.jpca.6b10526>

Please note:

Changes made as a result of publishing processes such as copy-editing, formatting and page numbers may not be reflected in this version. For the definitive version of this publication, please refer to the published source. You are advised to consult the publisher's version if you wish to cite this paper.

This version is being made available in accordance with publisher policies. See <http://orca.cf.ac.uk/policies.html> for usage policies. Copyright and moral rights for publications made available in ORCA are retained by the copyright holders.



# Chemical Equilibria and Kinetics in Aqueous Solutions of Zymonic Acid

Russell J. Perkins,<sup>†,‡</sup> Richard K. Shoemaker,<sup>†</sup> Barry K. Carpenter,<sup>§</sup> and Veronica Vaida<sup>\*,†,‡</sup>

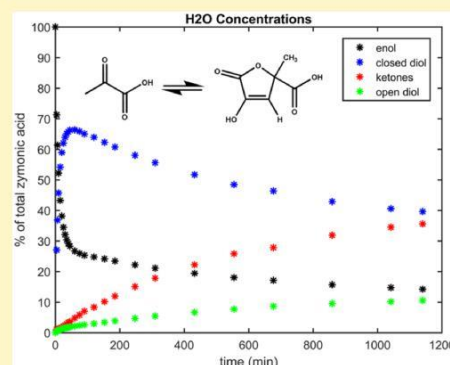
<sup>†</sup>Department of Chemistry and Biochemistry, University of Colorado at Boulder, UCB 215, Boulder, Colorado 80309, United States

<sup>‡</sup>Cooperative Institute for Research in Environmental Sciences, University of Colorado at Boulder, UCB 215, Boulder, Colorado 80309, United States

<sup>§</sup>School of Chemistry and the Physical Organic Chemistry Centre, Cardiff University, Cardiff CF10 3AT, United Kingdom

\* Supporting Information

**ABSTRACT:** The chemistry of pyruvic acid is of great interest due to its essential role in metabolism for all life and its role in atmospheric chemistry. Pyruvic acid under a wide range of conditions, including normal storage conditions, will spontaneously dimerize to form zymonic acid. We isolated zymonic acid and, using a variety of 1D and 2D NMR techniques, identified it as a single structure as a solid or dissolved in DMSO. When in aqueous solution, however, we identified a mixture of five different tautomers and hydrates in equilibrium with each other with no single dominant form. The kinetics of this conversion were studied *in situ* via NMR. The reactivity of the tautomers and hydrates in aqueous solution is investigated and discussed in terms of aqueous reaction mechanisms. There is strong evidence for a direct, reversible conversion from an enol to a geminal diol without passing through a ketone intermediate, which implies the reversible addition of water across a double bond under ambient conditions. Additionally, there is evidence for a base catalyzed lactone ring formation, which is in essence a base catalyzed esterification reaction. The equilibrium between pyruvic acid and its oligomers in aqueous solution is of consequence in the natural environment.



## INTRODUCTION

Pyruvic acid is a ubiquitous molecule in biology, where it takes an essential place at the core of metabolism for all life. It intersects anabolic and catabolic pathways that occur both aerobically and anaerobically, earning it a special place as a metabolite in both modern<sup>1</sup> and ancient life.<sup>2,3</sup> Additionally, it is an important molecule in the environment, particularly in the Earth's atmosphere,<sup>4-13</sup> and has even been found in carbonaceous meteorites.<sup>14</sup> In the atmosphere, formation of pyruvic acid oligomers or other high molecular weight compounds can be important for aerosol formation and processing.<sup>15-17</sup> The reactivity of pyruvic acid is important in these systems, and many studies have been carried out in an attempt to characterize reactive pathways involving pyruvic acid.<sup>18-35</sup> In many recent studies, however, the spontaneous dimerization of pyruvic acid is overlooked. It results in the formation of parapryruvic acid ( $\gamma$ -methyl- $\gamma$ -hydroxy- $\alpha$ -ketoglutarate) along with its lactone, zymonic acid ( $\alpha$ -keto- $\gamma$ -valerolactone- $\gamma$ -carboxylic acid). This "decomposition" was observed along with the first isolations of pyruvic acid by Berzelius in 1835<sup>36,37</sup> according to Wolff who, building on previous work,<sup>38-41</sup> produced the first correct structures and reasonable formation mechanisms around 1900.<sup>42-44</sup> Further investigations analyze the mechanism of formation as well as the structure of larger pyruvic acid polymers.<sup>45-48</sup>

Later studies are split between work examining metal catalysis<sup>49-52</sup> and biological processes.<sup>53-74</sup> Zymonic acid was

identified as a metabolite in yeast,<sup>53</sup> only to be shown to be a contaminant from pyruvic acid used, and an incorrect structure was first reported.<sup>54,55</sup> A number of other papers have discussed the detection or role of parapryruvic and zymonic acid in various biological contexts, including detection from living tissues and interactions with enzymes.<sup>56-74</sup> Interestingly, parapryruvic acid has been observed in meteorites alongside pyruvic acid<sup>14</sup> and discussed in the context of the origin of life.<sup>75</sup> There are several papers discussing the spontaneous formation of zymonic and parapryruvic acids from pyruvic acid under different conditions, which suggest that these molecules exist as contaminants in other experiments.<sup>55,76-79</sup> Because these dimerization products<sup>||</sup> are formed relatively easily, it is somewhat unclear whether previous detections of zymonic and parapryruvic acids are artifacts of the analytical techniques that were used.

The interconversion between the different forms of zymonic, parapryruvic, and pyruvic acids is especially interesting in aqueous solution and must be elucidated to achieve a full understanding of the aqueous phase chemistry of pyruvic acid. In this work, structural identification of different tautomers and hydrates of zymonic acid was performed using several different NMR techniques. At equilibrium under low pH conditions, we detect

and assign five different forms of pyruvic acid dimers in solution and investigate the mechanisms of their interconversion. Our higher resolution NMR work across a broader pH range allows for the differentiation of quickly exchanging species that were assigned to single components in most previous works.<sup>49–79</sup> We report identification and characterization of the pyruvic acid chemical dimerization products followed by a study of the kinetics of interconversion. Finally, potential mechanisms are discussed for the novel interconversions that are observed.

## RESULTS AND DISCUSSION

**Purification and Identification.** Pyruvic acid is the simplest  $\alpha$ -keto acid and, like most ketones, can convert between the ketone, enol, and geminal diol forms in aqueous solution.<sup>49,80</sup> For pyruvic acid, the ketone and geminal diol forms are thermodynamically favored in water and constitute the bulk of pyruvic acid with the ratio between them depending on solution conditions (pH, concentration, salt, and temperature). Likewise, parapyruvic acid is a keto acid and exists dominantly as either a ketone or geminal diol. Unlike pyruvic acid, it can undergo an intramolecular esterification reaction, resulting in the formation of a lactone. The lactone additionally has a ketone functionality and can exist in solution as a mixture of the ketone, geminal diol, and enol forms. The lactone enol of parapyruvic acid has been referred to as zymonic acid.

Zymonic acid appears to form spontaneously in pure liquid pyruvic acid samples or in aqueous solutions, likely through an aldol addition reaction.<sup>78</sup> This means that even very well-purified pyruvic acid will spontaneously convert to zymonic acid over time under normal storage conditions. In fact, several grams of crude zymonic acid were isolated via distillation from approximately 25 mL of pyruvic acid that had been stored at 4 °C for several months (see the [Experimental Section](#) for details). Further purification of zymonic acid was carried out in dry, aprotic solvents to preserve the purity and prevent the formation

of hydrates and ultimately resulted in a sticky, off-white powder which will be referred to as “purified zymonic acid”. Zymonic acid, both in crude and purified forms, smells strongly of caramel and is hygroscopic as well as solvoscopic.

NMR spectra of purified compounds were first taken in deuterated dimethyl sulfoxide (DMSO- $d_6$ ). The proton spectrum is shown in [Figure 1](#).

While the singlet peak at 6.25 ppm is strongly indicative of the enol form of this molecule and great care has been taken to avoid water contamination during purification, further evidence is required to rule out the corresponding molecule that has been hydrolyzed to create the open chain form. The open form would have an additional alcohol group as well as another acid group that should be visible in this spectrum. The broadness from peak 12 is likely due to exchange of the acid proton with water contamination in the DMSO, where peak 6, the enol proton, is not exchanging as quickly. This makes it unlikely that both peaks 12 and 6 are associated with carboxylic acids. It could be possible, although unlikely, for two carboxylic acid peaks to overlap, and perhaps for the alcohol peak to overlap with the peak from water contamination. The ratios of the peaks  $H^{12}:H^6:H^9:H^7$  are 1.17:1.06:1.00:2.92, which are in much better agreement for the closed form than the open one, however.  $^{13}C$  NMR spectra were taken for both the sample in DMSO- $d_6$  as well as the solid. Both spectra agree well with the structure of the closed enol form ([Supporting Information, Figure 12](#)).

NMR spectra were also taken in 10% deuterated water solutions and are shown in [Figure 2](#). Assignments were made through the use of a combination of NMR spectroscopies (COSY, HMBC, and HSQC; see [Supporting Information, Figures 1–11](#)). To a lesser extent, trends in chemical shift were used to differentiate between very similar molecules. For example, differentiating between the set of peaks assigned to the ketone and diol molecules was done by referencing the region in the carbon spectrum where geminal diols are generally found. Five different

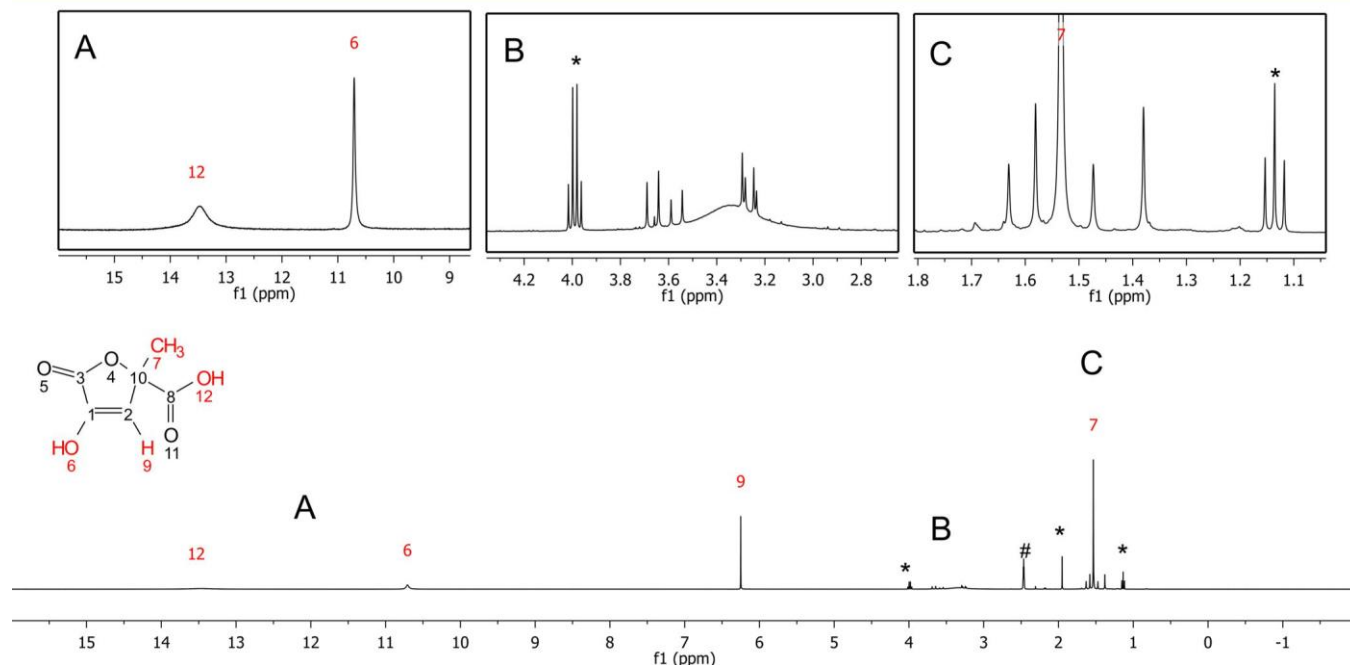


Figure 1.  $^1H$  NMR spectrum (400 MHz) of purified zymonic acid in DMSO- $d_6$  (bottom) with expanded spectral regions (top). Peaks numbered in red correlate with H atoms in the zymonic acid structure shown. \* indicates ethyl acetate impurity, and # indicates undeuterated DMSO. In box B, the broad peak at 3.35 ppm is water impurity due to the DMSO- $d_6$ .

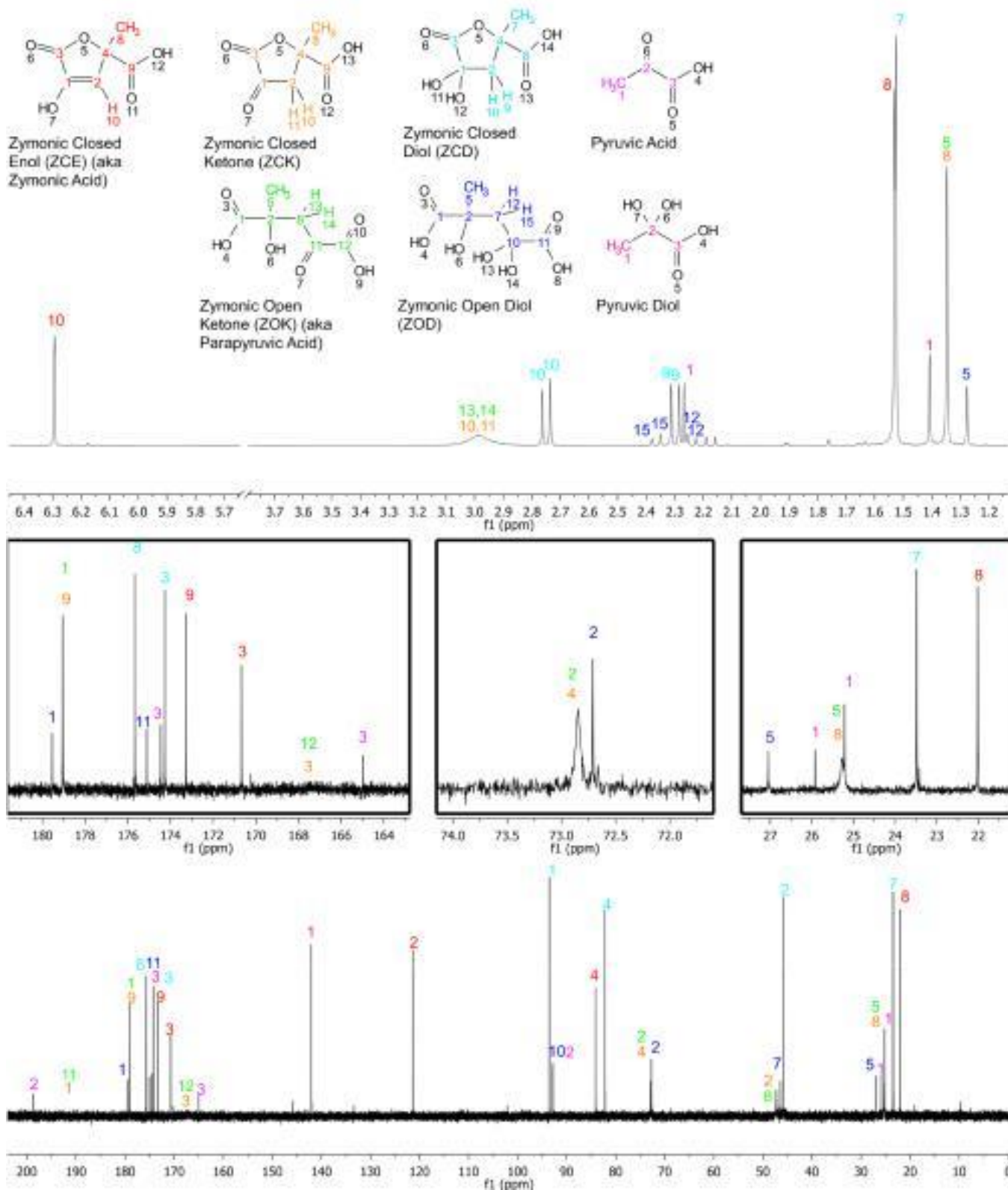


Figure 2.  $^1\text{H}$  (top) and  $^{13}\text{C}$  (bottom) NMR spectra (500 MHz) of zymonic acid in 10% deuterated water using WET water suppression with their corresponding structures. Peaks are labeled with the color and number corresponding to a carbon or group of equivalent hydrogens in the corresponding structures. The carbon NMR spectrum has been zoomed in at regions with overlapping peaks. Assignments of ZCK carbon 3 and ZOK carbon 12 are tentative, as they are expected to be very broad but somewhere in the region depicted.

species zymonic species are detected in equilibrium with each other in water and will be referred to as zymonic closed enol (ZCE), zymonic closed ketone (ZCK), zymonic open ketone

(ZOK, also known as parapyruvic acid), zymonic closed diol (ZCD), and zymonic open diol (ZOD). The nomenclature closed and open here refers to the cyclic and acyclic forms, respectively.

One compound that is expected from this chemistry but not assigned in Figure 2 is the aldol condensation product of pyruvic acid. This product would be ZOK (parapyruvic acid) with, using the atom labels found in Figure 2, OH 6 and H 13 or 14 removed via dehydration with a double bond appearing between carbons 2 and 8. The peaks at approximately 146 and 134 ppm in the carbon spectrum may be due to this aldol condensation product, but due to their relatively low abundance and lack of correlation in the 2D NMR spectra, a concrete assignment is not possible here.

There are several broad features in the spectra in Figure 2 which are associated with the two ketone forms of zymonic acid, ZOK and ZCK. These arise due to an exchange between the closed and open ring ketone forms, which appears to be in the intermediate exchange regime where chemical exchange occurs on the NMR time scale. Broader peaks are associated with atoms that are closest to the oxygens involved in ring formation. Peak width due to chemical exchange falls into several regimes based on the ratio of the exchange rate to the difference in resonance frequency of the exchanging species. When the exchange is very slow relative to the frequency difference, very little broadening occurs. As the exchange rate increases, the peaks associated with the exchanging species become increasingly broad and averaged until the coalescence point is reached, and faster exchange results in sharper peaks. The coalescence point occurs when the exchange rate  $k_c = \pi U/\sqrt{2}$ , where  $U$  is the frequency difference between the exchanging species. The observation that the peaks are broader where the largest chemical changes are occurring suggests that all the observed peaks are at or above the coalescence point. This was investigated further as a function of temperature and pH (Figure 3).

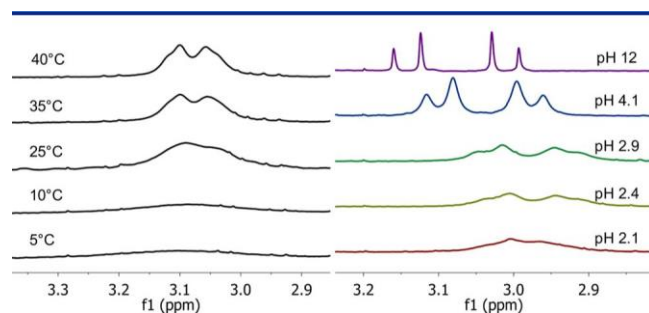


Figure 3. Comparison of CH<sub>2</sub> ketone proton NMR peaks as a function of temperature at unadjusted pH of 2.1 (left) and as a function of pH at 23 °C (right). The temperature dependent NMR spectra (left) were taken on an 800 MHz instrument, while the pH dependent spectra (right) were taken on a 500 MHz instrument.

The peaks in Figure 3 become sharper as temperature increases, clearly indicating that the CH<sub>2</sub> peak for ZOK/ZCK species are above coalescence or close to the coalescence temperature at 5 °C. This also results in broader peaks at 25 °C in the 800 MHz spectra compared to those in the 500 MHz spectra. The fact that the peaks become sharper with increasing pH indicates that the rate of exchange is increasing as a function of pH. This also indicates that the sharp peaks attributed to parapyruvic acid (ZOK here) in previous works are in fact due to two species in fast exchange, ZOK and ZCK. We approximate that this exchange rate is on the subsecond time scale in all cases as a very conservative estimate. Unfortunately, it is difficult to quantify the exchange rate without knowing the frequency difference between the exchanging species. This is generally measured in the slow exchange limit but is inaccessible for this

system in water as it would require temperatures below the freezing point or the addition of large quantities of strong acid, which become problematic both due to reactivity and for the measurement of comparable spectra. While problematic, it is also extremely interesting that relatively fast exchange between ZOK and ZCK occurs across all pH and temperature conditions for liquid water at ambient pressure.

With these forms of zymonic acid identified, infrared spectra were taken of the zymonic acid ZCE form both as the crude product and the purified powder (Figure 4). The crude product includes a significant amount of pyruvic acid, which may be acting as a solvent. The initial spectrum obtained, therefore, has a large pyruvic acid absorption. The pyruvic acid absorption is subtracted using the known spectrum for pyruvic acid.<sup>81</sup> Because the quantity of pyruvic acid was not well characterized in the crude product (and changes over time), subtraction was carried out to eliminate the peak at 1350 cm<sup>-1</sup> that is due to pyruvic acid and in a reasonably clear region of the zymonic acid spectrum. This procedure is supported by the fact that the second spectrum, taken of purified powder in a KBr pellet, does not exhibit the peak at 1350 cm<sup>-1</sup>. The IR spectra are very similar between the subtracted crude product and the purified product, further suggesting that the crude product exists in the ZCE structure. The peak at 1660 cm<sup>-1</sup> is likely the C=C enol stretch, lending additional support to this assignment.

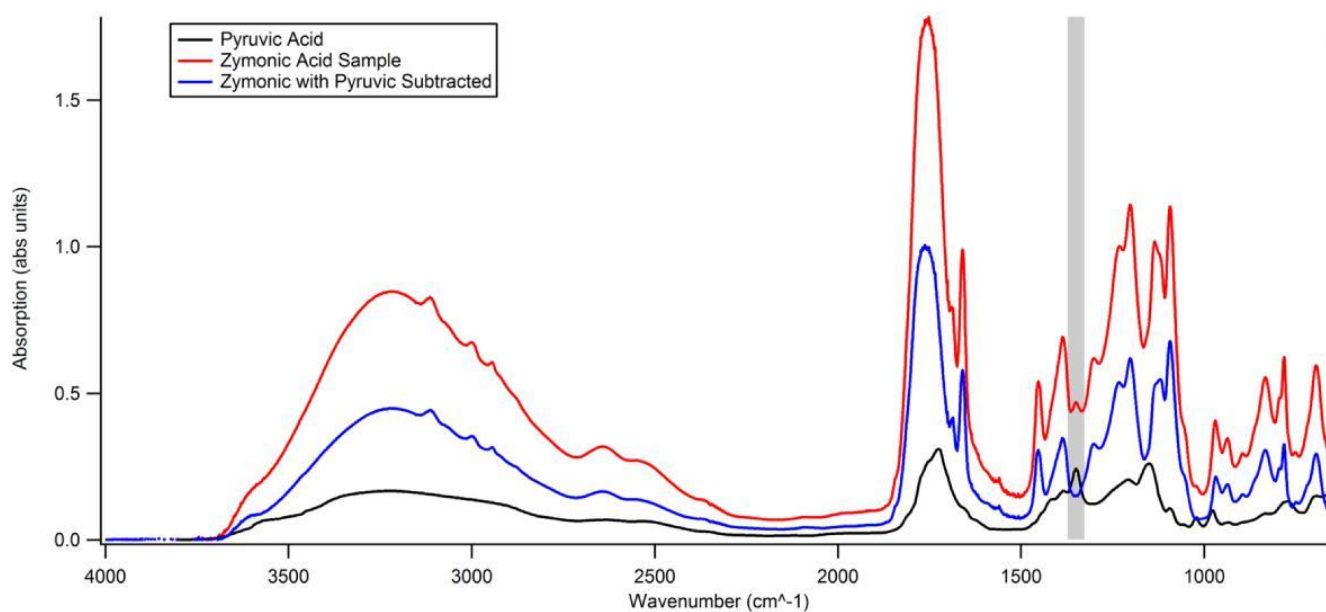
**Aqueous Interconversions.** With the structures well identified, the interconversions between the different forms in aqueous solution were investigated. Because the solid form is almost entirely the closed enol initially, conversion to the other forms can be monitored using NMR after mixing with 90% water and 10% D<sub>2</sub>O (Figure 5). Immediately following mixing, there is a decrease in the enol form and a corresponding increase in the closed diol form. Quasi-equilibrium appears to be reached around 25 min after mixing with about 62% closed diol and 35% enol with less than 5% total other forms. At longer times, the enol and closed diol forms decrease concurrently as the ketone and open diol forms grow in. The short time data suggest that a transformation from the enol directly to the closed diol form is occurring, which would correlate with the regioselective addition of water across the enol double bond. This is further evidenced by quickly decreasing UV absorption as a function of time immediately following mixing (Supporting Information, Figure 13).

Additional information can be gained by monitoring mixing with 100% D<sub>2</sub>O because the carbons alpha to a ketone group can exchange upon reaction from a ketone to an enol. The methyl hydrogens, however, do not exchange. This allows simultaneous observation of the change in relative abundance of zymonic species and the deuteration of each species (Figure 6).

The same trend is observed with much slower rates of transformation. The slowing of rates is at least partially due to a kinetic isotope effect, as most of the transformations between zymonic species involve hydrogen or deuterium movement. The equilibrium ratios between species are shifted slightly in D<sub>2</sub>O as well, which is not unexpected given the drastic changes to the kinetics. The deuteration percentages calculated for low time points are clearly erroneous for species that have very low abundance: the ketone and the open diol. Because the deuteration kinetics will depend on both forward and backward reaction rates, fitting this data should allow for their extraction. First, a full kinetic fit was performed using a relatively simple model allowing for exchange between most species, shown in Scheme 1.

Using this kinetic scheme to fit only the water data works well, but there is not enough information to successfully fit both

A



B

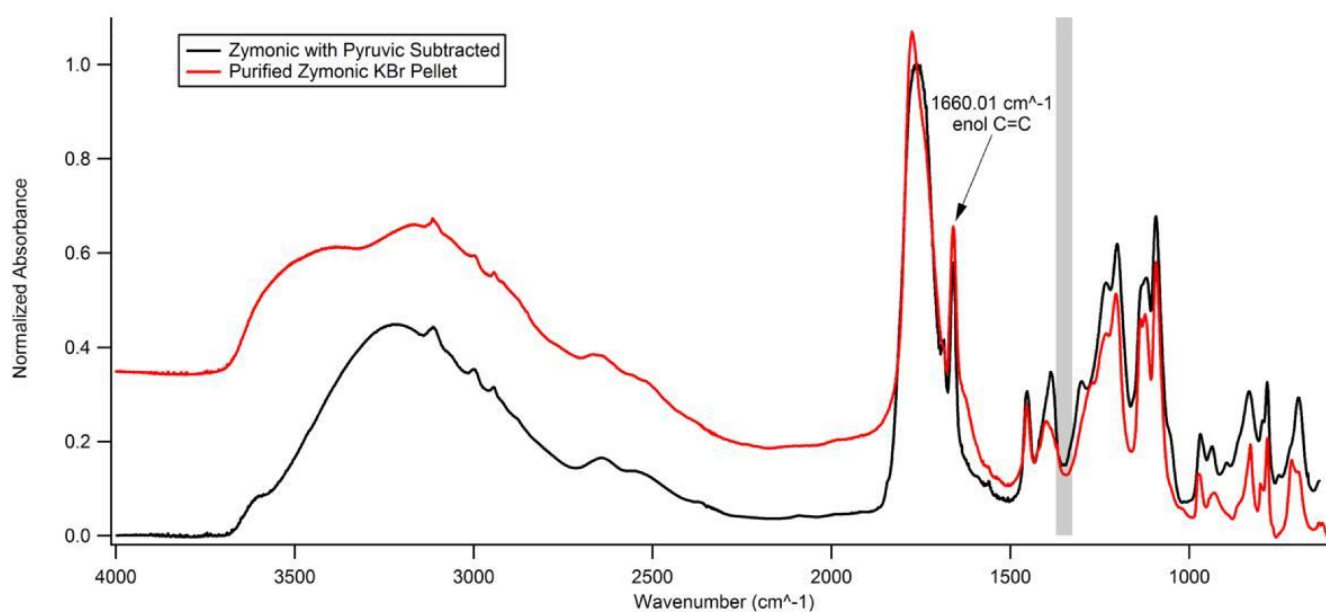


Figure 4. Infrared spectra of (A) crude zymonic acid spread on a NaCl window (red), pyruvic acid<sup>82</sup> (black), and zymonic acid with the pyruvic acid contamination subtracted. (B) Comparison of zymonic closed enol (ZCE) spectra taken in panel A and a spectrum of purified zymonic acid in a KBr pellet. The gray region highlights the area where the pyruvic acid peak is subtracted away.

forward and backward rate constants with a high degree of certainty. When considering the deuteration experiment, however, there are a few observations that necessitate modification of this simple scheme. The peaks from the ZCD methylene protons (labeled as 9 and 10 in light blue in Figure 2) exhibit a geminal splitting due to the chiral center on the adjacent quaternary carbon (labeled as 4 in light blue in Figure 2). These peaks are associated with two different isomers, one with the acid group *syn* to the hydrogen and one *anti* (10 and 9 in light blue in Figure 2). While it is tempting to assign the downfield peaks as the *syn*-conformation, this simple analysis is often misleading. When one of the methylene hydrogens is replaced with a deuterium, the geminal coupling becomes much weaker, resulting in a single resolvable peak associated with the *syn*- or *anti*- conformations of ZCD. For the D<sub>2</sub>O mixing experiment, the only methylene peaks that are observed for the ZCD and ZOD appear as singlets, indicating a minimum of 50% deuteration for these species

(see Supporting Information, Figure 14). This is expected, given the initial ZCE form requires the addition of a water molecule in order to transition into any of the other forms. The more interesting observation, however, is that the *syn*- and *anti*-ZCD peaks do not grow at the same rate. Although the peaks have not been assigned to one conformer or the other, there is certainly a stereoselective mechanism at work. This may be due to intramolecular acid catalysis, which has previously been described for different molecular systems.<sup>83–85</sup>

The D<sub>2</sub>O mixing data can be fit simultaneously with the water mixing data to Scheme 2.

It should be noted that the rate constants in Scheme 2 labeled k<sub>1</sub>–k<sub>7</sub> all involve the movement of deuterium instead of hydrogen. Because of this, these rate constants are not expected to be the same as the corresponding rate constants in water, which involves movement of hydrogens. k<sub>-2H</sub> is the exception to this because it involves the loss of a hydrogen to the solvent and

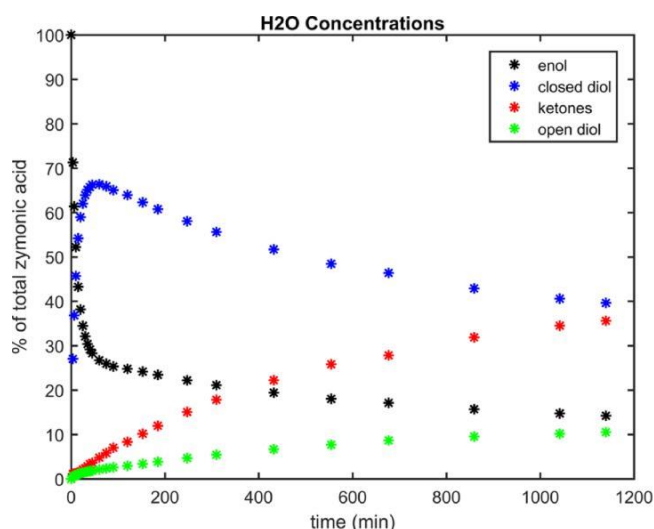


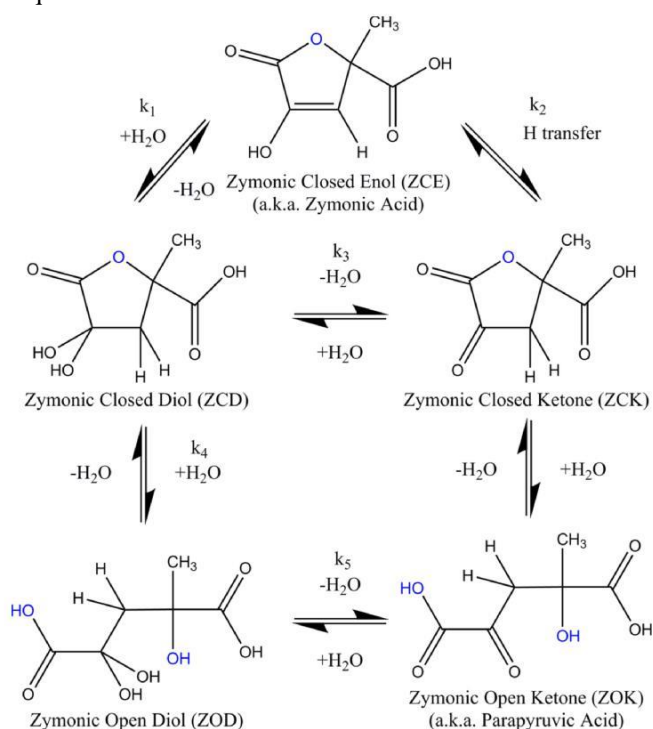
Figure 5. Changes in zymonic acid structures after mixing with 90% water and 10% D<sub>2</sub>O measured in situ with NMR.

should be identical to the  $k_{-2}$  in Scheme 2. The fits agree very well with the experimental data. Fits and rate constants are shown in Figure 7.

While many of these reaction rates are likely to depend on the solution pH and therefore the concentration of zymonic acid, there is interesting mechanistic information present from this data under one set of conditions. Rather than the conventional ketone-enol tautomerism, the enol reacts relatively quickly with water to form the geminal diol (as ZCD). The reverse reaction from ZCD to ZCE happens readily as well. The conventional reaction mechanism for an enol under acidic conditions that could lead to the formation of diol is shown in Scheme 3. This mechanism takes advantage of intramolecular acid catalysis to activate the enol.<sup>83-85</sup>

At the branch point shown in Scheme 3, to match the experimental observation that the diol is formed preferentially over the ketone, it is required in this mechanism that the nucleophilic attack by water occurs much more quickly than the deprotonation of the ketone. This is something that is very difficult to justify, as it requires either an energetic barrier to

Scheme 1. Schematic of the Simple Kinetic Model for the Observed Conversion of Zymonic Acid Structures in Aqueous Solution<sup>a</sup>



<sup>a</sup>Rate constants for the conversion in water are shown with the closest arrow indicating the forward direction. Oxygens/OH groups involved in ring formation are highlighted in blue.

deprotonation or for water to be an exceptionally strong nucleophile in this situation. Neither of these requirements seem likely, so the mechanism shown in Scheme 3 is unlikely to occur, but why? There does not seem to be an obvious reason why the conventional chemistry should be forbidden.

There is a stark contrast between the reaction rates for the ring forming/opening reactions of the ketones and diols. The conversion between the closed and open ketone forms is by far the fastest reaction observed with a rate constant in the subsecond

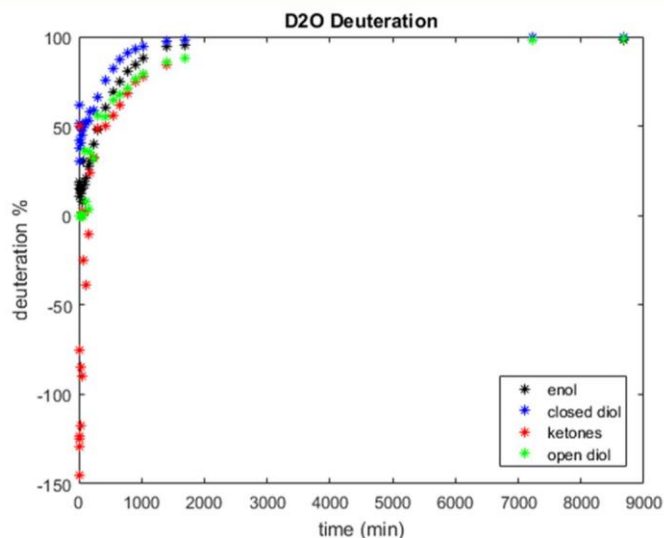
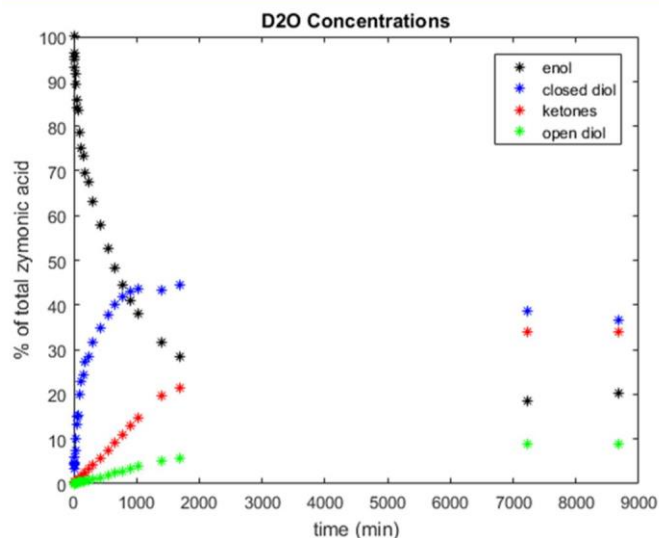
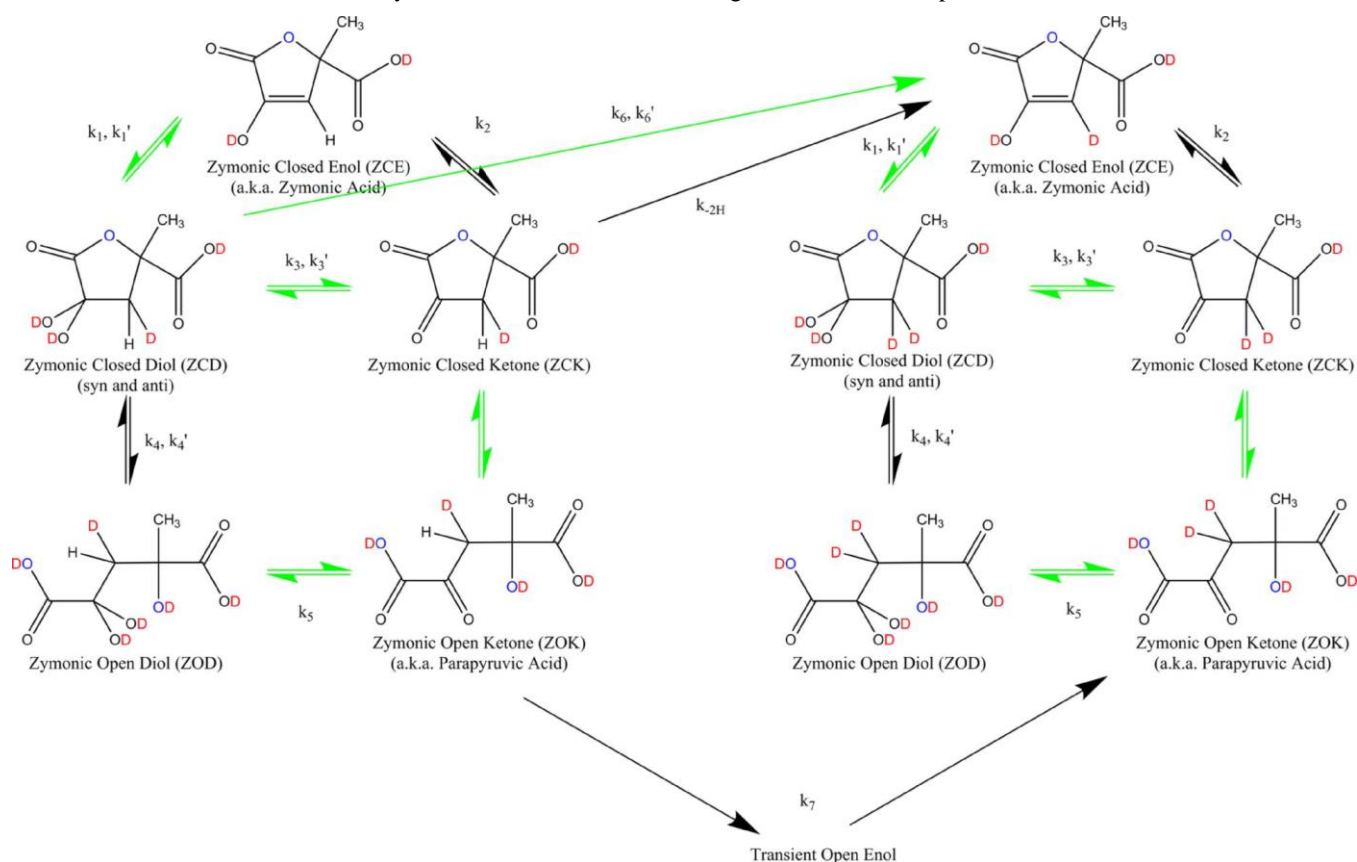


Figure 6. Change in zymonic acid structure (left) and deuteration (right) after mixing with 100% D<sub>2</sub>O.

Scheme 2. Interconversion between Zymonic Acid Forms and Resulting Deuteration for Experiments Mixed with 100% D<sub>2</sub>O<sup>a</sup>



<sup>a</sup>Reaction rate constants are associated with the arrow closest to them being the forward direction. Identically numbered rate constants that are differentiated by priming (i.e.  $k_1$  and  $k_1'$ ) are for reaction rates of different stereoisomers. Rate constant  $k_{-2H}$  is the rate constant for ZCK to ZCE observed in the water mixing experiment and effectively couples the systems together. Steps  $k_6$ ,  $k_6'$ ,  $k_7$ , and  $k_{-2H}$  are all expected to be effectively irreversible due to the very low abundance of H<sub>2</sub>O in solution. Arrows in green indicate the dominant pathways.

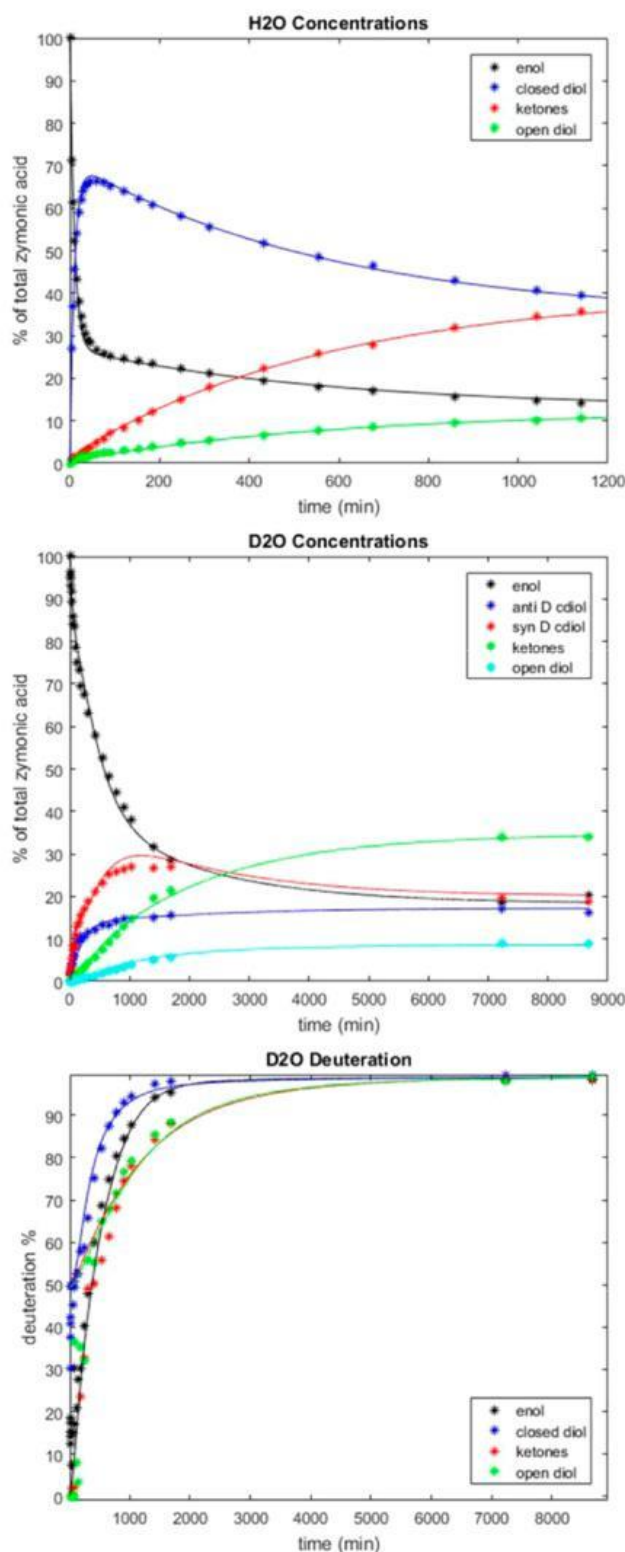
range rather than minutes or hours. The rate constant for the opening on the cyclic geminal diol (ZCD to ZOD) directly is at least 6 orders of magnitude slower. The formation of the lactone ring is expected to proceed via an esterification reaction which involves the protonation of the carboxylic carbonyl oxygen followed by nucleophilic attack on the carbonyl carbon by a hydroxyl group. In contrast to this conventional reaction mechanism, however, this reaction proceeds faster for the zymonic ketones under increasingly basic conditions, as evidenced by the movement further from coalescence and into the fast exchange regime for the CH<sub>2</sub> resonances in Figure 3 discussed earlier. This is extremely unusual, as it constitutes a base catalyzed esterification reaction, which is commonly accepted not to occur. While it is unclear what mechanisms explain the interesting chemistry that is occurring, they certainly are not the standard, expected mechanisms. There is, however, compelling evidence that these transitions between ZCE and ZCD as well as ZCK and ZOK are occurring, and the latter rate increases with increasing pH.

## CONCLUSIONS

In this work, zymonic acid was isolated, purified, and identified as a single component system as a solid or dissolved in DMSO. In aqueous solution, however, it is a complex, interconverting, multicomponent system. One and two-dimensional NMR measurements were carried out and supplemented by pH, field, and temperature dependent NMR studies. These measurements

were used to assign all the major components observed in aqueous solution as well as gather kinetic data for their interconversion in water and D<sub>2</sub>O. The fastest interconversion appears to be between the cyclic and acyclic ketone forms of zymonic acid (ZCK and ZOK) on the subsecond time scale. This rate of interconversion increases with increasing pH, which has caused the mixture of these two substances to be misidentified as a single substance in previous literature.<sup>49–79</sup> The slower kinetic interconversions in water indicate the direct transition from an enol to a geminal diol (ZCE to ZCD) without a ketone intermediate. A kinetic fit was performed that reinforces the validity of this observation. Two reaction paths were observed that contrast established mechanistic literature. To our knowledge, this is the first time that either a base catalyzed esterification or a direct enol to geminal diol hydration has been observed. We have not proposed mechanisms for this unconventional chemistry.

The existence of these compounds may be important to current or past biology as contaminants or possibly metabolites. There is evidence that in modern biology there are enzymes that catalyze the conversion of zymonic acid (likely an open chain form) to pyruvic acid.<sup>64,65,67,70</sup> This may arise due to structural similarities to native substrates, although there have been reports of inhibition of the tricarboxylic acid cycle<sup>60,61</sup> as well as anti-malarial effects of zymonic acid.<sup>59</sup> Other detections of zymonic acid, usually in the ZOK form or the transaminated amino acid derivative, have been made in various biological systems.<sup>57,58,71,72</sup> It is unclear exactly what role zymonic acid plays in these systems,



	lower bound ( $\text{min}^{-1}$ )	upper bound ( $\text{min}^{-1}$ )
$k_{w1}$	$6.98^{-02}$	$7.19^{-02}$
$k_{w-1}$	$2.69^{-02}$	$2.83^{-02}$
$k_{w2}$	$5.47^{-11}$	$1.57^{-06}$
$k_{w-2}$	$1.68^{-09}$	$9.44^{-04}$
$k_{w3}$	$2.38^{-03}$	$3.22^{-03}$
$k_{w-3}$	$4.36^{-05}$	$3.41^{-04}$
$k_{w4}$	$5.02^{-09}$	$3.97^{-04}$
$k_{w-4}$	$8.94^{-05}$	$3.45^{-03}$
$k_{w5}$	$9.58^{-02}$	$1.53^{-01}$
$k_{w-5}$	$3.20^{-01}$	$4.99^{-01}$
$k_{d1}$	$6.42^{-04}$	$8.27^{-04}$
$k_{d-1}$	$1.13^{-10}$	$7.26^{-04}$
$k_{d1}'$	$2.85^{-03}$	$3.09^{-03}$
$k_{d-1}'$	$2.97^{-03}$	$3.56^{-03}$
$k_{d2}$	$5.90^{-12}$	$2.50^{-04}$
$k_{d-2}$	$1.20^{-13}$	$7.07^{-09}$
$k_{d3}$	$3.49^{-04}$	$1.96^{-03}$
$k_{d-3}$	$2.62^{-10}$	$9.30^{-04}$
$k_{d3}'$	$8.97^{-14}$	$6.09^{-09}$
$k_{d-3}'$	$7.62^{-13}$	$1.32^{-05}$
$k_{d4}$	$3.44^{-04}$	$7.87^{-04}$
$k_{d-4}$	$5.10^{-12}$	$3.37^{-03}$
$k_{d4}'$	$2.26^{-13}$	$1.61^{-08}$
$k_{d-4}'$	$4.17^{-04}$	$1.83^{-03}$
$k_{d5}$	$4.24^{-11}$	$1.20^{-03}$
$k_{d-5}$	$1.30^{-05}$	$1.28^{-03}$
$k_{d6}$	$6.64^{-04}$	$1.83^{-03}$
$k_{d6}'$	$1.33^{-02}$	$1.46^{-02}$
$k_{d7}$	$1.53^{-13}$	$1.03^{-08}$

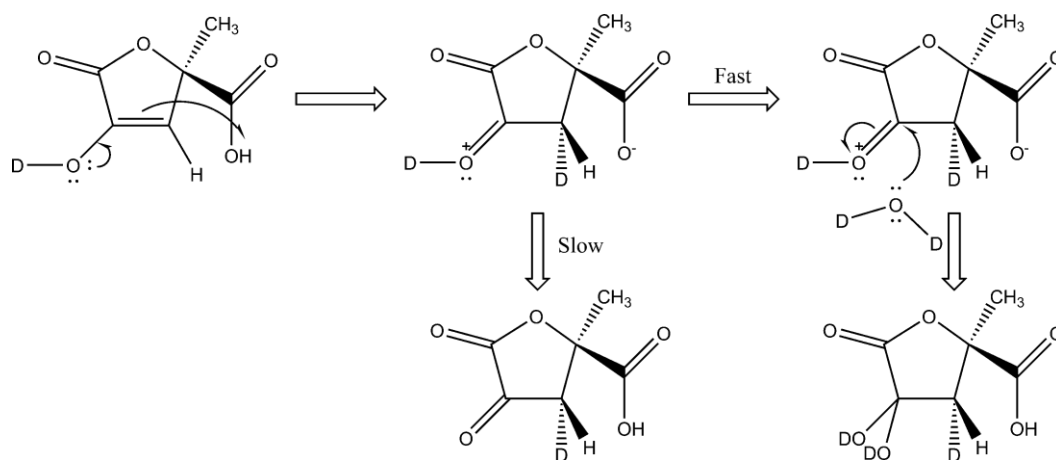
Figure 7. Left: Experimental data (markers) and calculated fits (lines) for relative abundance of different zymonic acid forms over time for  $\sim 0.1$  mM

solutions in water and D<sub>2</sub>O as well as the deuteration of each species over time in D<sub>2</sub>O. Right: Calculated forward and backward rate constants for each reaction shown in Scheme 2 with  $k_w$  and  $k_d$  values indicating reaction rates in water and D<sub>2</sub>O, respectively. The range of each value is the 95% confidence interval calculated through bootstrap resampling. Shading in red indicates values that had not converged well after 2145 resamples with bound changes greater than 5% with the addition of 100 resample values to the statistical pool. The cell shaded in blue is at the upper bound for the fit and may be even larger.

but the coexistence between different structural forms in aqueous solutions that we clarify will be vital to understanding its behavior.

In atmospheric chemistry, these pyruvic dimers may also play a role in aerosol processing or formation, especially given their observed extreme hygroscopicity. Aerosol particles have an

Scheme 3. Conventional Reaction Mechanism Based on Acid Catalyzed Enol Chemistry Resulting in the Formation of ZCD from ZCE and the Required Relative Rates of Reaction at the Branch Point to Match Experimental Data



important impact on human health as well as climate, where they impact radiative forcing and act as condensation nuclei. Secondary organic aerosol (SOA) is formed in the atmosphere through gas or condensed phase reactions that often produce low volatility oligomers.<sup>9,17,86–93</sup> Aqueous phases provide effective and interesting reaction environments for organic oligomer formation and contribute to the SOA budget.<sup>93–100</sup> The aqueous phase reactions that are most studied are oxidation by ozone<sup>10</sup> or hydroxyl radicals<sup>101–105</sup> as well as photochemical reactions.<sup>35,98,106–110</sup> The ability of pyruvic acid to dimerize may be a particularly relevant dark reaction for SOA formation due to the properties of the dimers examined here.

## EXPERIMENTAL SECTION

**Purification.** Crude zymonic acid was isolated from ~25 mL of pyruvic acid (Sigma-Aldrich, 98%) that had been stored at 4 °C for several months by distillation. Distillation was carried out at 70 °C and 400 mTorr for several hours until the bulk of the pyruvic acid was removed. Upon completion of distillation, several grams of a viscous yellow liquid remained that smelled strongly of caramel. Upon cooling, this yellow substance became extremely viscous and was a sticky, glassy solid at 4 °C. This substance was identified as mainly zymonic acid via NMR and will be referred to as crude zymonic acid with approximately 10–20% pyruvic acid remaining and several unidentified impurities. Crude zymonic acid (125 mg) was dissolved in approximately 1 mL of ethyl acetate (Mallinckrodt, ≥99.5%) and then exposed to 0.5 mmHg vacuum for several hours. About 450 mg of ethyl acetate remained, and the sample became very viscous. The ethyl acetate was then extracted with excess hexanes (Sigma-Aldrich, ≥99%) facilitated by water bath sonication. Hexane supernatant was discarded, and vacuum was applied to remove residual solvent. This process was repeated several times to obtain an off-white sticky powder.

**NMR.** <sup>1</sup>H, COSY, HMBC, and HSQC spectra were obtained at 23 °C using a Varian INOVA-500 NMR spectrometer operating at 499.60 MHz for <sup>1</sup>H observation. To perform NMR with <sup>1</sup>H detection in aqueous solution, WET solvent suppression was used to eliminate >99% of the H<sub>2</sub>O signal.<sup>111</sup> In all cases (1D and 2D), <sup>1</sup>H detection experiments were performed using an optimized WET water suppression as the initial preparation step of the NMR pulse sequence. The two-dimensional gradient-selected heteronuclear single-bond correlation spectrum using matched adiabatic pulse (2D-gHSQCad) experiments were

performed with matched adiabatic sweeps for coherence transfer, corresponding to a central <sup>13</sup>C–<sup>1</sup>H J value of 146 Hz.<sup>112</sup> Gradient-selected heteronuclear multiple bond correlation using adiabatic pulse (gHMBCad) experiments were optimized for a long-range <sup>13</sup>C–<sup>1</sup>H coupling constant of 8.0 Hz. Gradient-selected homonuclear correlation spectroscopy (gCOSY) was performed with two 90° pulses and variable evolution time between them.

Temperature dependent spectra were acquired using a Varian/Agilent VNMRS/DD2 800 MHz NMR operating at 798.6 mHz for <sup>1</sup>H detection.

Solid-state <sup>13</sup>C CPMAS NMR experiments were performed using a Varian INOVA-400 NMR spectrometer operating at 400.16 MHz for <sup>1</sup>H observation. The probe used in these experiments is a Varian 2-channel 4 mm CPMAS probe modified with a new spinning module and coil designed and constructed by Revolution NMR, LLC in Fort Collins, CO. This probe utilizes Zirconia “pencil” style rotors and is capable of spinning 4 mm rotors stably at spinning frequencies up to 18 kHz. <sup>13</sup>C CPMAS experiments were performed using a 3.3 μs <sup>1</sup>H 90° pulse, employing ramped cross-polarization with a spin-lock field centered at a magnitude 67 kHz. The contact time used was 4.0 ms, optimized for maximum polarization transfer with minimal signal loss due to T<sub>1ρ</sub> relaxation. A delay of 3.0 s was employed to allow for <sup>1</sup>H relaxation between scans. Broadband TPPM (time-proportional phase modulation) <sup>1</sup>H decoupling was applied during signal acquisition, utilizing a CW decoupling power of 75 kHz. Magic angle spinning (MAS) was performed at 13.1 kHz.

**FTIR.** Fourier transform infrared spectroscopy was performed using a Bruker Tensor 27 spectrometer for crude samples and a Thermo-Nicolet Avatar 360 spectrometer for powder samples. Crude samples were prepared by spreading crude zymonic acid on NaCl windows and were scanned with 1 cm<sup>-1</sup> resolution averaged over 100 scans. Powder samples were mixed with KBr (>99%, Sigma-Aldrich) and pressed into transparent discs using a pellet press. These samples were scanned with 1 cm<sup>-1</sup> resolution and averaged over 64 scans.

**UV-vis.** Purified zymonic acid was mixed with 18.2 MΩ water and immediately scanned using a Varian (Agilent) Cary 5000 spectrometer with a 0.1 s average time, 1 nm data interval, and a 0.5 nm spectral bandwidth. Scans were taken periodically and tracked by the time elapsed since zymonic dissolution.

**Kinetic Fit.** NMR kinetic data was first analyzed in MestReNova v10.0.2–15465 by fitting assigned peaks to generalized

Lorentzian line shapes and extracting relative peak areas from the fit areas for each time step. The kinetic data were modeled in MATLAB R2016a (9.0.0.341360) using a full set of differential equations for all reaction pathways described. Rate constants were simultaneously optimized by minimizing uncertainty-weighted deviation of the fit from the experimental data using the built-in constrained optimization function `fmincon`. Error estimates for rate constants were generated by randomizing input kinetic data as a Gaussian distribution within experimental uncertainty and refitting, generating a statistical pool of rate constants. Average values are not reported because the statistical pools are, for many rate constants, highly non-Gaussian.

## ASSOCIATED CONTENT

### \* Supporting Information

The Supporting Information is available free of charge on the ACS Publications website

Raw NMR FIDs (ZIP)  
Tabulated kinetic and FTIR data (ZIP)  
2D NMR spectra, solid state NMR spectra, and UV-visible absorbance spectra (PDF)

## AUTHOR INFORMATION

### Corresponding Author

\*E-mail: [Vaida@colorado.edu](mailto:Vaida@colorado.edu); Phone: 303-492-8605; Fax: 303-492-5894.

### ORCID

Veronica Vaida: 0000-0001-5863-8056

### Notes

The authors declare no competing financial interest.

## ACKNOWLEDGMENTS

R.J.P. and V.V. would like to acknowledge support from a CIRES Innovative Research Proposal, NSF CHE 1306386, and NASA Habitable Worlds grant NNX15AP20G. R.J.P. acknowledges support from the NIH/CU Molecular Biophysics Training Program.

## ADDITIONAL NOTE

For convenience, in this work we will refer to all the six carbon molecules we observe as pyruvic acid dimerization products even though they appear to be produced through a variety of hydration and isomerization reactions. Included in this category are zymonic acid and parapyruvic acid.

## REFERENCES

- (1) Voet, D.; Voet, J. G. *Biochemistry*, 4th ed. Binder Ready Version; Wiley: Hoboken, NJ, 2010.
- (2) Griffith, E. C.; Shoemaker, R. K.; Vaida, V. *Sunlight-Initiated Chemistry of Aqueous Pyruvic Acid: Building Complexity in the Origin of Life. Origins Life Evol. Biospheres* 2013, 43 (4-5), 341-352.
- (3) Cody, G. D.; Boctor, N. Z.; Filley, T. R.; Hazen, R. M.; Scott, J. H.; Sharma, A.; Yoder, H. S. *Primordial Carbonylated Iron-Sulfur Compounds and the Synthesis of Pyruvate. Science* 2000, 289 (5483), 1337-1340.
- (4) Kawamura, K. Identification of C2-C10 Omega-Oxocarboxylic Acids, Pyruvic Acid, and C2-C3 Alpha-Dicarbonyls in Wet Precipitation and Aerosol Samples by Capillary GC and GC/MS. *Anal. Chem.* 1993, 65 (23), 3505-3511.
- (5) Sempere, R.; Kawamura, K. Comparative Distributions of Dicarboxylic Acids and Related Polar Compounds in Snow, Rain and Aerosols from Urban Atmosphere. *Atmos. Environ.* 1994, 28 (3), 449-459.
- (6) Kawamura, K.; Kasukabe, H.; Barrie, L. A. Source and Reaction Pathways of Dicarboxylic Acids, Ketoacids and Dicarbonyls in Arctic Aerosols: One Year of Observations. *Atmos. Environ.* 1996, 30 (10-11), 1709-1722.
- (7) Fu, P.; Zhuang, G.; Sun, Y.; Wang, Q.; Chen, J.; Ren, L.; Yang, F.; Wang, Z.; Pan, X.; Li, X.; et al. Molecular Markers of Biomass Burning, Fungal Spores and Biogenic SOA in the Taklimakan Desert Aerosols. *Atmos. Environ.* 2016, 130, 64-73.
- (8) Brooks Avery, G., Jr.; Willey, J. D.; Kieber, R. J. Diurnal Variations in Major Rainwater Components at a Coastal Site in North Carolina. *Atmos. Environ.* 2001, 35 (23), 3927-3933.
- (9) Altieri, K. E.; Carlton, A. G.; Lim, H.-J.; Turpin, B. J.; Seitzinger, S. P. Evidence for Oligomer Formation in Clouds: Reactions of Isoprene Oxidation Products. *Environ. Sci. Technol.* 2006, 40 (16), 4956-4960.
- (10) Nguyen, T. B.; Bateman, A. P.; Bones, D. L.; Nizkorodov, S. A.; Laskin, J.; Laskin, A. High-Resolution Mass Spectrometry Analysis of Secondary Organic Aerosol Generated by Ozonolysis of Isoprene. *Atmos. Environ.* 2010, 44 (8), 1032-1042.
- (11) Veres, P. R.; Roberts, J. M.; Cochran, A. K.; Gilman, J. B.; Kuster, W. C.; Holloway, J. S.; Graus, M.; Flynn, J.; Lefer, B.; Warneke, C.; et al. Evidence of Rapid Production of Organic Acids in an Urban Air Mass. *Geophys. Res. Lett.* 2011, 38 (17), L17807.
- (12) Warneck, P. Multi-Phase Chemistry of C2 and C3 Organic Compounds in the Marine Atmosphere. *J. Atmos. Chem.* 2005, 51 (2), 119-159.
- (13) Guenther, A. Biological and Chemical Diversity of Biogenic Volatile Organic Emissions into the Atmosphere. *ISRN Atmospheric Sci.* 2013, 2013, 1-27.
- (14) Cooper, G.; Reed, C.; Nguyen, D.; Carter, M.; Wang, Y. Detection and Formation Scenario of Citric Acid, Pyruvic Acid, and Other Possible Metabolism Precursors in Carbonaceous Meteorites. *Proc. Natl. Acad. Sci. U. S. A.* 2011, 108 (34), 14015-14020.
- (15) Charlson, R. J.; Seinfeld, J. H.; Nenes, A.; Kulmala, M.; Laaksonen, A.; Facchini, M. C. Reshaping the Theory of Cloud Formation. *Science* 2001, 292 (5524), 2025-2026.
- (16) Ellison, G. B.; Tuck, A. F.; Vaida, V. Atmospheric Processing of Organic Aerosols. *J. Geophys. Res. Atmospheres* 1999, 104 (D9), 11633-11641.
- (17) Donaldson, D. J.; Vaida, V. The Influence of Organic Films at the Air-Aqueous Boundary on Atmospheric Processes. *Chem. Rev.* 2006, 106 (4), 1445-1461.
- (18) Vesley, G. F.; Leermakers, P. A. The Photochemistry of  $\alpha$ -Keto Acids and  $\alpha$ -Keto Esters. III. Photolysis of Pyruvic Acid in the Vapor Phase. *J. Phys. Chem.* 1964, 68 (8), 2364-2366.
- (19) Closs, G. L.; Miller, R. J. Photoreduction and Photodecarboxylation of Pyruvic Acid. Applications of CIDNP to Mechanistic Photochemistry. *J. Am. Chem. Soc.* 1978, 100 (11), 3483-3494.
- (20) Colberg, M. R.; Watkins, R. J.; Krogh, O. D. Vibrationally Excited Carbon Dioxide Produced by Infrared Multiphoton Pyrolysis. *J. Phys. Chem.* 1984, 88 (13), 2817-2821.
- (21) Yamamoto, S.; Back, R. A. The Photolysis and Thermal Decomposition of Pyruvic Acid in the Gas Phase. *Can. J. Chem.* 1985, 63 (2), 549-554.
- (22) Taylor, R. The Mechanism of Thermal Eliminations Part XXIII: [1] The Thermal Decomposition of Pyruvic Acid. *Int. J. Chem. Kinet.* 1987, 19 (8), 709-713.
- (23) Saito, K.; Sasaki, G.; Okada, K.; Tanaka, S. Unimolecular Decomposition of Pyruvic Acid: An Experimental and Theoretical Study. *J. Phys. Chem.* 1994, 98 (14), 3756-3761.
- (24) Stefan, M. I.; Bolton, J. R. Reinvestigation of the Acetone Degradation Mechanism in Dilute Aqueous Solution by the UV/H2O2 Process. *Environ. Sci. Technol.* 1999, 33 (6), 870-873.
- (25) Mellouki, A.; Mu, Y. On the Atmospheric Degradation of Pyruvic Acid in the Gas Phase. *J. Photochem. Photobiol., A* 2003, 157 (2-3), 295-300.
- (26) Carlton, A. G.; Turpin, B. J.; Lim, H.-J.; Altieri, K. E.; Seitzinger, S. Link between Isoprene and Secondary Organic Aerosol (SOA): Pyruvic Acid Oxidation Yields Low Volatility Organic Acids in Clouds. *Geophys. Res. Lett.* 2006, 33 (6), L06822.

- (27) Takahashi, K.; Plath, K. L.; Skodje, R. T.; Vaida, V. Dynamics of Vibrational Overtone Excited Pyruvic Acid in the Gas Phase: Line Broadening through Hydrogen-Atom Chattering. *J. Phys. Chem. A* 2008, 112 (32), 7321–7331.
- (28) Plath, K. L.; Takahashi, K.; Skodje, R. T.; Vaida, V. Fundamental and Overtone Vibrational Spectra of Gas-Phase Pyruvic Acid. *J. Phys. Chem. A* 2009, 113 (26), 7294–7303.
- (29) Rincon, A. G.; Guzman, M. I.; Hoffmann, M. R.; Colussi, A. J. Optical Absorptivity versus Molecular Composition of Model Organic Aerosol Matter. *J. Phys. Chem. A* 2009, 113 (39), 10512–10520.
- (30) Larsen, M. C.; Vaida, V. Near Infrared Photochemistry of Pyruvic Acid in Aqueous Solution. *J. Phys. Chem. A* 2012, 116 (24), 5840–5846.
- (31) Reed Harris, A. E.; Ervens, B.; Shoemaker, R. K.; Kroll, J. A.; Rapf, R. J.; Griffith, E. C.; Monod, A.; Vaida, V. Photochemical Kinetics of Pyruvic Acid in Aqueous Solution. *J. Phys. Chem. A* 2014, 118 (37), 8505–8516.
- (32) da Silva, G. Decomposition of Pyruvic Acid on the Ground State Potential Energy Surface. *J. Phys. Chem. A* 2015, 120 (2), 276.
- (33) Asmus, C.; Mozziconacci, O.; Schöneich, C. Low-Temperature NMR Characterization of Reaction of Sodium Pyruvate with Hydrogen Peroxide. *J. Phys. Chem. A* 2015, 119 (6), 966–977.
- (34) Lopalco, A.; Dalwadi, G.; Niu, S.; Schowen, R. L.; Douglas, J.; Stella, V. J. Mechanism of Decarboxylation of Pyruvic Acid in the Presence of Hydrogen Peroxide. *J. Pharm. Sci.* 2016, 105 (2), 705–713.
- (35) Griffith, E. C.; Carpenter, B. K.; Shoemaker, R. K.; Vaida, V. Photochemistry of Aqueous Pyruvic Acid. *Proc. Natl. Acad. Sci. U. S. A.* 2013, 110 (29), 11714.
- (36) Berzelius, J. J. Ueber Die Destillationsproducte Der Trauben-saurē. *Ann. Phys.* 1835, 112 (9), 1–29.
- (37) Berzelius, J. J. On Dry Distilled Racemic Acid. *Acta Chem. Scand.* 1960, 14, 1677–1680.
- (38) Völckel, C. Ueber Die Producte Der Destillation Der Weinsaurē. *Justus Liebigs Ann. Chem.* 1854, 89 (1), 57–76.
- (39) Finck, C. Ueber Die Zersetzung Der Brenztraubensaurē Durch Baryhydrat. *Justus Liebigs Ann. Chem.* 1862, 122 (2), 182–191.
- (40) Böttinger, C. Beitrag Zur Kenntniss Der Brenztraubensaurē. *Justus Liebigs Ann. Chem.* 1877, 188 (3), 293–342.
- (41) Serda, R. Beiträge Zur Kenntniss Der Pyrotitersaurē. Ph.D. Thesis, Kaiser-Wilhelm University of Strassburg, 1889.
- (42) Wolff, L. I. Ueber Die Synthese Der Uvitinsäure Aus Brenztraubensaurē. *Justus Liebigs Ann. Chem.* 1899, 305 (2), 125–153.
- (43) Wolff, L., II Ueber Die Parabrenztraubensaurē. *Justus Liebigs Ann. Chem.* 1899, 305 (2), 154–165.
- (44) Wolff, L. Ueber Ein Neues Condensationsproduct Der Brenztraubensaurē. *Justus Liebigs Ann. Chem.* 1901, 317 (1), 1–22.
- (45) de Jong, A. W. K. Les Transformations Des Sels de L'acide Pyruvique. *Recl. Trav. Chim. Pays-Bas Belg.* 1901, 20 (10), 365–387.
- (46) Wille, F. Die Synthese Der 1,4-Diketoadipinsaurē Und Ihre Biologische Bedeutung. *Justus Liebigs Ann. Chem.* 1939, 538 (1), 237–260.
- (47) Waldmann, E.; Prey, V.; Jelinek, F. Zur Kenntnis der Brenztraubensaurē. *Monatshefte Für Chem. Verwandte Teile Anderer Wiss.* 1954, 85 (4), 872–881.
- (48) Prey, V.; Waldmann, E.; Berbalk, H. Zur Kenntnis der Brenztraubensaurē. *Monatsh. Chem.* 1955, 86 (3), 408–413.
- (49) Leussing, D.; Stanfield, C. K. A Nuclear Magnetic Resonance Study of Aqueous Pyruvate-Glycinate-Zinc(II) and Related Systems. *J. Am. Chem. Soc.* 1964, 86 (14), 2805–2810.
- (50) Tallman, D. E.; Leussing, D. L. Pyruvate Dimerization Catalyzed by nickel(II) and zinc(II). I. Equilibrium with nickel(II) and zinc(II). *J. Am. Chem. Soc.* 1969, 91 (23), 6253–6256.
- (51) Tallman, D. E.; Leussing, D. L. Pyruvate Dimerization Catalyzed by nickel(II) and zinc(II). II. Kinetics. *J. Am. Chem. Soc.* 1969, 91 (23), 6256–6262.
- (52) Lin, H.-L.; Yu, Y.-O.; Jwo, J.-J. Kinetic Study of the Ce(III)-, Mn(II)-, or Ferriin-Catalyzed Belousov-Zhabotinsky Reaction with Pyruvic Acid. *Int. J. Chem. Kinet.* 2000, 32 (7), 408–418.
- (53) Stodola, F. H.; Shotwell, O. L.; Lockwood, L. B. Zymonic Acid, a New Metabolic Product of Some Yeasts Grown in Aerated Culture. I. Structure Studies. *J. Am. Chem. Soc.* 1952, 74 (21), 5415–5418.
- (54) Bloomer, J. L.; Gross, M. A. Biosynthesis of Zymonic Acid in *Trichosporon Capitatum*. *J. Chem. Soc. D* 1970, 73–74.
- (55) Bloomer, J. L.; Gross, M. A.; Kappler, F. E.; Pandey, G. N. Identity of "zymonic Acid" with a Pyruvate Derivative. *J. Chem. Soc. D* 1970, 0, 1030a–1030a.
- (56) Krebs, H. A.; Johnson, W. A. Acetopyruvic Acid (Alphagamma-Diketovaleic Acid) as an Intermediate Metabolite in Animal Tissues. *Biochem. J.* 1937, 31 (5), 772–779.
- (57) Virtanen, A. I.; Berg, A.-M.; Risberg, E.; Lamm, O. New Aminodicarboxylic Acids and Corresponding Alpha-Keto Acids in *Phyllitis Scolopendrium*. *Acta Chem. Scand.* 1955, 9, 553–554.
- (58) Grobbelaar, N.; Pollard, J. K.; Steward, F. C. New Soluble Nitrogen Compounds (Amino- and Imino-Acids and Amides) in Plants. *Nature* 1955, 175 (4460), 703–708.
- (59) Trager, W.; Singer, I. An Antimalarial Effect in Vitro of Parapyruvic Acid. *Exp. Biol. Med.* 1955, 90 (2), 539–542.
- (60) Montgomery, C. M.; Webb, J. L. Detection of a New Inhibitor of the Tricarboxylic Acid Cycle. *Science* 1954, 120 (3125), 843–844.
- (61) Montgomery, C. M.; Webb, J. L. Metabolic Studies on Heart Mitochondria II. the Inhibitory Action of Parapyruvate on the Tricarboxylic Acid Cycle. *J. Biol. Chem.* 1956, 221 (1), 359–368.
- (62) Montgomery, C. M.; Webb, J. L. Metabolic Studies on Heart Mitochondria I. the Operation of the Normal Tricarboxylic Acid Cycle in the Oxidation of Pyruvate. *J. Biol. Chem.* 1956, 221 (1), 347–358.
- (63) Stradner, A.; Sedgwick, H.; Cardinaux, F.; Poon, W. C. K.; Egelhaaf, S. U.; Schurtenberger, P. Equilibrium Cluster Formation in Concentrated Protein Solutions and Colloids. *Nature* 2004, 432 (7016), 492–495.
- (64) Marcus, A.; Shannon, L. M.  $\gamma$ -Methyl- $\gamma$ -Hydroxy- $\alpha$ -Ketoglutaric Aldolase II. STUDIES WITH PYRUVATE-C<sup>14</sup>. *J. Biol. Chem.* 1962, 237 (11), 3348–3353.
- (65) Shannon, L. M.; Marcus, A.  $\gamma$ -Methyl- $\gamma$ -Hydroxy- $\alpha$ -Ketoglutaric Aldolase I. PURIFICATION AND PROPERTIES. *J. Biol. Chem.* 1962, 237 (11), 3342–3347.
- (66) Kobes, R. D.; Dekker, E. Variant Properties of Bovine Liver 2-Keto-4-Hydroxyglutarate Aldolase; Its  $\beta$ -Decarboxylase Activity, Lack of Substrate Stereospecificity, and Structural Requirements for Binding Substrate Analogs. *Biochim. Biophys. Acta BBA - Enzymol.* 1971, 250 (1), 238–250.
- (67) Tack, B. F.; Chapman, P. J.; Dagley, S. Purification and Properties of 4-Hydroxy-4-Methyl-2-Oxoglutarate Aldolase. *J. Biol. Chem.* 1972, 247 (20), 6444–6449.
- (68) Herbert, J. D.; Coulson, R. A.; Hernandez, T.; Ehrensvar, G. A. Carbonic Anhydrase Requirement for the Synthesis of Glutamine from Pyruvate in the Chameleon. *Biochem. Biophys. Res. Commun.* 1975, 65 (3), 1054–1060.
- (69) Maruyama, K. Enzymes Responsible for Degradation of 4-Oxalomesaconic Acid in *Pseudomonas Ochraceae*. *J. Biochem. (Tokyo)* 1983, 93 (2), 567–574.
- (70) Ohshima, T.; Hoshino, T.; Ikarashi, T. Isolation and Structure of a New Organic Acid Accumulated in Tulip Plant (*Tulipa Gesnerioides*). *Soil Sci. Plant Nutr.* 1988, 34 (1), 75–86.
- (71) Winter, H. C.; Dekker, E. E. Specificity of Aspartate Amino-transferases from Leguminous Plants for 4-Substituted Glutamic Acids. *Plant Physiol.* 1989, 89 (4), 1122–1128.
- (72) Maruyama, K. Purification and Properties of 4-Hydroxy-4-Methyl-2-Oxoglutarate Aldolase from *Pseudomonas Ochraceae* Grown on Phthalate. *J. Biochem. (Tokyo)* 1990, 108 (2), 327–333.
- (73) Helaine, V.; Rossi, J.; Gefflaut, T.; Alaux, S.; Bolte, J. Synthesis of 4,4-Disubstituted L-Glutamic Acids by Enzymatic Transamination. *Adv. Synth. Catal.* 2001, 343 (6–7), 692–697.
- (74) Xian, M.; Alaux, S.; Sagot, E.; Gefflaut, T. Chemoenzymatic Synthesis of Glutamic Acid Analogues: Substrate Specificity and Synthetic Applications of Branched Chain Aminotransferase from *Escherichia Coli*. *J. Org. Chem.* 2007, 72 (20), 7560–7566.

- (75) Novikov, Y.; Copley, S. D. Reactivity Landscape of Pyruvate under Simulated Hydrothermal Vent Conditions. *Proc. Natl. Acad. Sci. U. S. A.* 2013, 110 (33), 13283–13288.
- (76) Goldfine, H. The Formation of  $\gamma$ -Hydroxy- $\gamma$ -Methylglutamic Acid from a Common Impurity in Pyruvic Acid. *Biochim. Biophys. Acta* 1960, 40, 557–559.
- (77) Buldain, G.; Santos, C. D. L.; Frydman, B. Carbon-13 Nuclear Magnetic Resonance Spectra of the Hydrate, Keto and Enol Forms of Oxalacetic Acid. *Magn. Reson. Chem.* 1985, 23 (6), 478–481.
- (78) Margolis, S. A.; Coxon, B. Identification and Quantitation of the Impurities in Sodium Pyruvate. *Anal. Chem.* 1986, 58 (12), 2504–2510.
- (79) Fell, L. M.; Francis, J. T.; Holmes, J. L.; Terlouw, J. K. The Intriguing Behaviour of (Ionized) Oxalacetic Acid Investigated by Tandem Mass Spectrometry. *Int. J. Mass Spectrom. Ion Processes* 1997, 165, 179–194.
- (80) Pocker, Y.; Meany, J. E.; Nist, B. J.; Zadorojny, C. Reversible Hydration of Pyruvic Acid. I. Equilibrium Studies. *J. Phys. Chem.* 1969, 73 (9), 2879–2882.
- (81) NIST. Mass Spec Data Center, Infrared Spectra. In NIST Chemistry WebBook, NIST Standard Reference Database Number 69; Linstrom, P.J., Mallard, W.G., Eds.; National Institute of Standards and Technology: Gaithersburg, MD, 2016.
- (82) The Coblentz Society Desk Book of Infrared Spectra, 2nd ed; Carver, C.D., Ed.; The Coblentz Society: Kirkwood, MO, 1982.
- (83) Kirby, A. J.; Meyer, G. Intramolecular Catalysis by the Ionised Carboxy-Group of the Hydrolysis of Enol Esters, and of the General Acid Catalysed Ketonisation of the Enols Produced. *J. Chem. Soc., Perkin Trans. 2* 1972, 1446.
- (84) Kirby, A. J.; O'Carroll, F. Highly Efficient Intramolecular General Acid Catalysis of Enol Ether Hydrolysis, with Rapid Proton Transfer to Carbon. *J. Chem. Soc., Perkin Trans. 2* 1994, 649.
- (85) Kirby, A. J.; Williams, N. H. Efficient Intramolecular General Acid Catalysis of Enol Ether Hydrolysis. Hydrogen-Bonding Stabilisation of the Transition State for Proton Transfer to Carbon. *J. Chem. Soc., Perkin Trans. 2* 1994, 643.
- (86) Finlayson-Pitts, B. J. Reactions at Surfaces in the Atmosphere: Integration of Experiments and Theory as Necessary (but Not Necessarily Sufficient) for Predicting the Physical Chemistry of Aerosols. *Phys. Chem. Chem. Phys.* 2009, 11, 7760–7779.
- (87) Martins-Costa, M. T. C.; Anglada, J. M.; Francisco, J. S.; Ruiz-Lopez, M. F. Reactivity of Volatile Organic Compounds at the Surface of a Water Droplet. *J. Am. Chem. Soc.* 2012, 134, 11821–11827.
- (88) Rudich, Y.; Donahue, N. M.; Mentel, T. F. Aging of Organic Aerosol: Bridging the Gap between Laboratory and Field Studies. *Annu. Rev. Phys. Chem.* 2007, 58, 321–352.
- (89) Carlton, A. G.; Wiedinmyer, C.; Kroll, J. H. A Review of Secondary Organic Aerosol (SOA) Formation from Isoprene. *Atmos. Chem. Phys.* 2009, 9, 4987–5005.
- (90) Thornton, D. C. O.; Brooks, S. D.; Chen, J. Protein and Carbohydrate Exopolymer Particles in the Sea Surface Microlayer (SML). *Front. Mar. Sci.* 2016, 3, 135.
- (91) McNeill, V. F. Aqueous Organic Chemistry in the Atmosphere: Sources and Chemical Processing of Organic Aerosols. *Environ. Sci. Technol.* 2015, 49 (3), 1237–1244.
- (92) Ebben, C. J.; Strick, B. F.; Upshur, M. A.; Chase, H. M.; Achtyl, J. L.; Thomson, R. J.; Geiger, F. M. Towards the Identification of Molecular Constituents Associated with the Surfaces of Isoprene-Derived Secondary Organic Aerosol (SOA) Particles. *Atmos. Chem. Phys.* 2014, 14 (5), 2303–2314.
- (93) Lienhard, D. M.; Bones, D. L.; Zuend, A.; Krieger, U. K.; Reid, J. P.; Peter, T. Measurements of Thermodynamic and Optical Properties of Selected Aqueous Organic and Organic-Inorganic Mixtures of Atmospheric Relevance. *J. Phys. Chem. A* 2012, 116 (40), 9954–9968.
- (94) Herrmann, H.; Tilgner, A.; Barzaghi, P.; Majdik, Z.; Gligorovski, S.; Poulain, L.; Monod, A. Towards a More Detailed Description of Tropospheric Aqueous Phase Organic Chemistry: CAPRAM 3.0. *Atmos. Environ.* 2005, 39, 4351–4363.
- (95) Epstein, S. A.; Nizkorodov, S. A. A Comparison of the Chemical Sinks of Atmospheric Organics in the Gas and Aqueous Phase. *Atmos. Chem. Phys.* 2012, 12, 8205–8222.
- (96) Bregonzio-Rozier, L.; Giorio, C.; Siekmann, F.; Pangu, E.; Morales, S. B.; Temime-Roussel, B.; Gratien, A.; Michoud, V.; Cazaunau, M.; DeWitt, H. L.; et al. Secondary Organic Aerosol Formation from Isoprene Photooxidation during Cloud Condensation-Evaporation Cycles. *Atmos. Chem. Phys.* 2016, 16, 1747–1760.
- (97) Galloway, M. M.; Powelson, M. H.; Sedehi, N.; Wood, S. E.; Millage, K. D.; Kononenko, J. A.; Rynaski, A. D.; De Haan, D. O. Secondary Organic Aerosol Formation during Evaporation of Droplets Containing Atmospheric Aldehydes, Amines, and Ammonium Sulfate. *Environ. Sci. Technol.* 2014, 48 (24), 14417–14425.
- (98) Sun, Y. L.; Zhang, Q.; Anastasio, C.; Sun, J. Insights into Secondary Organic Aerosol Formed via Aqueous-Phase Reactions of Phenolic Compounds Based on High Resolution Mass Spectrometry. *Atmos. Chem. Phys.* 2010, 10 (10), 4809–4822.
- (99) Bones, D. L.; Reid, J. P.; Lienhard, D. M.; Krieger, U. K. Comparing the Mechanism of Water Condensation and Evaporation in Glassy Aerosol. *Proc. Natl. Acad. Sci. U. S. A.* 2012, 109 (29), 11613–11618.
- (100) Avzianova, E.; Brooks, S. D. Raman Spectroscopy of Glyoxal Oligomers in Aqueous Solutions. *Spectrochim. Acta, Part A* 2013, 101, 40–48.
- (101) Ervens, B.; Sorooshian, A.; Lim, Y. B.; Turpin, B. J. Key Parameters Controlling OH-Initiated Formation of Secondary Organic Aerosol in the Aqueous Phase (aqSOA). *J. Geophys. Res.-Atmospheres* 2014, 119, 3997–4016.
- (102) Monod, A.; Poulain, L.; Grubert, S.; Voisin, D.; Wortham, H. Kinetics of OH-Initiated Oxidation of Oxygenated Organic Compounds in the Aqueous Phase: New Rate Constants, Structure-Activity Relationships and Atmospheric Implications. *Atmos. Environ.* 2005, 39, 7667–7688.
- (103) Lim, Y. B.; Tan, Y.; Turpin, B. J. Chemical Insights, Explicit Chemistry, and Yields of Secondary Organic Aerosol from OH Radical Oxidation of Methylglyoxal and Glyoxal in the Aqueous Phase. *Atmos. Chem. Phys.* 2013, 13, 8651–8667.
- (104) Claeys, M.; Graham, B.; Vas, G.; Wang, W.; Vermeylen, R.; Pashynska, V.; Cafmeyer, J.; Guyon, P.; Andreae, M. O.; Artaxo, P.; et al. Formation of Secondary Organic Aerosols through Photooxidation of Isoprene. *Science* 2004, 303, 1173–1176.
- (105) Kroll, J. H.; Lim, C. Y.; Kessler, S. H.; Wilson, K. R. Heterogeneous Oxidation of Atmospheric Organic Aerosol: Kinetics of Changes to the Amount and Oxidation State of Particle-Phase Organic Carbon. *J. Phys. Chem. A* 2015, 119, 10767–10783.
- (106) Fu, H.; Ciuraru, R.; Dupart, Y.; Passaniti, M.; Tinel, L.; Rossignol, S.; Perrier, S.; Donaldson, D. J.; Chen, J.; George, C. Photosensitized Production of Atmospherically Reactive Organic Compounds at the Air/Aqueous Interface. *J. Am. Chem. Soc.* 2015, 137 (26), 8348–8351.
- (107) Guzman, M. I.; Colussi, A. J.; Hoffmann, M. R. Photoinduced Oligomerization of Aqueous Pyruvic Acid. *J. Phys. Chem. A* 2006, 110, 3619–3626.
- (108) George, C.; Ammann, M.; D'Anna, B.; Donaldson, D. J.; Nizkorodov, S. A. Heterogeneous Photochemistry in the Atmosphere. *Chem. Rev.* 2015, 115 (10), 4218–4258.
- (109) Rossignol, S.; Aregahegn, K. Z.; Tinel, L.; Fine, L.; Nozriere, B.; George, C. Glyoxal Induced Atmospheric Photosensitized Chemistry Leading to Organic Aerosol Growth. *Environ. Sci. Technol.* 2014, 48 (6), 3218–3227.
- (110) Bateman, A. P.; Nizkorodov, S. A.; Laskin, J.; Laskin, A. Photolytic Processing of Secondary Organic Aerosols Dissolved in Cloud Droplets. *Phys. Chem. Chem. Phys.* 2011, 13 (26), 12199–12212.
- (111) Ogg, R. J.; Kingsley, P. B.; Taylor, J. S. WET, a T1- and B1-Insensitive Water-Suppression Method for in Vivo Localized <sup>1</sup>H NMR Spectroscopy. *J. Magn. Reson., Ser. B* 1994, 104 (1), 1–10.
- (112) Boyer, R. D.; Johnson, R.; Krishnamurthy, K. Compensation of Refocusing Inefficiency with Synchronized Inversion Sweep (CRISIS) in Multiplicity-Edited HSQC. *J. Magn. Reson.* 2003, 165 (2), 253–259.